Available online at www.sciencedirect.com
ScienceDirect
International Journal of Pharmaceutics 357 (2008) 85–94
INTERNATIONAL JOURNAL OF PHARMACEUTICS
www.elsevier.com/locate/ijpharm

Preclinical characterization of intestinal absorption and metabolism of promising anti-Alzheimer's dimer bis(7)-tacrine

Li Zhang [a], Hua Yu [a,b], Wen Ming Li [a], Man Chun Cheung [a], Yuan Ping Pang [c], Ze Ming Gu [d], Kelvin Chan [e], Yi Tao Wang [b], Zhong Zuo [f,*], Yi Fan Han [g,**]

[a] *Department of Biochemistry, Hong Kong University of Science & Technology, Clear Water Bay, Kowloon, Hong Kong, SAR, PR China*
[b] *Institute of Chinese Medical Sciences, University of Macau, Macau, SAR, PR China*
[c] *Computer-Aided Molecular Design Laboratory, Mayo Clinic College of Medicine, 200 First Street SW, Rochester, MN, USA*
[d] *XenoBiotic Laboratories, Inc., Plainsboro, NJ, USA*
[e] *School of Applied Sciences, University of Wolverhampton, United Kingdom*
[f] *School of Pharmacy, Faculty of Medicine, Chinese University of Hong Kong, Shatin, N.T., Hong Kong, SAR, PR China*
[g] *Department of Applied Biology and Chemical Technology, The Hong Kong Polytechnic University, Hung Hom, Kowloon, Hong Kong, SAR, PR China*

Received 16 October 2007; accepted 21 January 2008
Available online 2 February 2008

Abstract

The present study aims to investigate the preclinical intestinal absorption of bis(7)-tacrine (B7T) using different absorption models. In addition, potential intestinal and liver first-pass metabolism was evaluated by in vitro incubation of B7T with rat intestine and liver microsome. Results showed that the permeability of B7T across artificial membrane was pH dependent with rapid diffusion achieved at both pH 6.8 and 7.4. However, the absorptive permeability of B7T in Caco-2 cell model was substantially lower than that in the artificial membrane accompanied with over 56% of B7T being trapped within Caco-2 cells. In the rat in situ intestinal perfusion model, B7T was subject to an extensive intestinal extraction (>90%) with extremely low concentration of B7T detected in mesenteric blood, which was further found to be associated with the high tissue binding (99.9%) of B7T. In vitro incubation of B7T with rat liver and intestinal microsomes revealed that hydroxylation of B7T might mainly occur in rat liver rather than intestine. In conclusion, B7T is expected to have a low oral bioavailability in vivo, which may be due to its poor intestinal permeability, significant tissue binding and hepatic hydroxylation metabolism.

Keywords: Bis(7)-tacrine; Intestinal absorption; Metabolism

1. Introduction

Alzheimer's disease (AD) is a progressive neurodegenerative disease characterized by deterioration of cognitive function, dementia, memory loss, and altered behavior (Tariot, 2001; Bird, 1998). Acetylcholinesterase inhibitors (AChEIs), which could increase the amount and residence time of acetylcholine at acetylcholine receptors within the brain, are the most effective medications for the treatment of AD (Wilkinson et al., 2004). Since the mid-'90s, only four AChEIs, namely tacrine (marketed by Parke-Davis as Cognex® in 1993), E2020 or donepezil (marketed by Pfizer as Aricept® in 1996), rivastigmine (marketed by Norvatis as Exelon® in 2000) and galantamine (marked by Shire as Reminyl® in 2001), have been approved by the FDA in the US for the treatment of AD (Standridge, 2004). Among the AChEIs investigated, Tacrine, donepezil, galantamine and physostigmine are reversible inhibitors of acetylcholinesterase and butyrylcholinesterase, while metrifonate is considered to be an irreversible inhibitor and rivastigmine a pseudoirreversible inhibitor. Among all the commercially available AChEIs, tacrine is the first one approved for the therapy of AD. However, it is no longer extensively used in clinical practice due to its hepatotoxicity (Watkins et al., 1994). In addition peripheral cholinergic adverse effects are common for the cholinesterase inhibitors with an incidence ranging 7–30% (Nordberg and Svensson, 1998). Therefore, there is a need to search for alternative AChEIs that could lower the incidence of the above side effects.

* Corresponding author. Tel.: +86 852 26096832; fax: +86 852 26035295.
** Corresponding author. Tel.: +86 852 34008695; fax: +86 852 23649932.
E-mail addresses: joanzuo@cuhk.edu.hk (Z. Zuo), Yifan.HAN@inet.polyu.edu.hk (Y.F. Han).

0378-5173/$ – see front matter © 2008 Published by Elsevier B.V.
doi:10.1016/j.ijpharm.2008.01.037

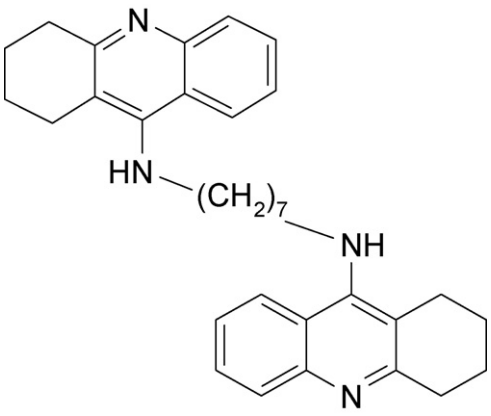

Fig. 1. Chemical structure of B7T.

Bis(7)-tacrine (B7T), a dimeric tacrine analog, is designed with aid of computer docking program and synthesized by our research group as a novel acetylcholinesterase inhibitor for the treatment of AD (Fig. 1). A series of our previous studies have demonstrated that B7T is much more potent and selective on acetylcholinesterase than tacrine (Wang et al., 1999; Xiao et al., 2000; Wu et al., 2000). Moreover, B7T was recently found to be able to protect against glutamate-induced neurotoxicity (Li et al., 2005) and inhibit nitric oxide synthase (Li et al., 2006). These recent findings from us also revealed that these novel AChEIs concurrently possess the NMDAR/NO signaling blocking activity, which might serve as one of the most effective therapeutic strategies to slowdown the neurodegeneration in addition to improving the cognitive functions for the prevention and treatment of AD.

In order to explore the further development of B7T for animal and human clinical studies, there is an urge to investigate its biopharmaceutics and pharmacokinetics characteristics. Since oral route still remains the most desirable and convenient route of administration for new chemical entities including the currently available anti-AD drugs such as donepezil, galantamine, rivastigmine, we plan to first investigate whether B7T could become an oral administered drug like other AChEIs.

Various in vitro and in situ models have been used to screen for the oral absorption of drug candidates. Among them, the parallel artificial membrane permeation assay (PAMPA), Caco-2 cell monolayer model, and rat single-pass intestinal perfusion model are the most commonly used. PAMPA has the advantages of being relatively cheap, less labor intensive, reproductive and capable of evaluating drug permeability in a wide range of pH. However, artificial membrane cannot provide any information on the metabolism and carrier-mediated transport of drug candidates due to its non-cell based nature. Unlike the artificial membranes, Caco-2 monolayer model consists of Caco-2 cells that are derived from human colon carcinoma. Though the enzyme expression in Caco-2 cells was generally reported to be lower than that in intestinal tissue (Sun et al., 2002; Paine and Fisher, 2000), efflux transporters such as P-gp, MRPs and MXR family were expressed in Caco-2 cells (Saitoh and Aungst, 1995; Hirohashi et al., 2000; Gutmann et al., 2005). The transporter-mediated efflux activity could be thus estimated in Caco-2 monolayer model by comparing the bi-directional permeability of the drug candidates. In addition to the in vitro model, rat singe-pass intestinal perfusion model is developed as an in situ model, which is considered to be the most close to in vivo situation in terms of the expression of enzymes and transporters. The rate and extent of intestinal absorption of drugs are usually estimated by determining the disappearance of the drugs in the perfusate or the drugs appearance in the mesenteric blood (Cummins et al., 2003; Johnson et al., 2003). In addition to intestinal permeability, hepatic and intestinal metabolism is usually one of the major contributors to the extent of oral bioavailabilities of drugs. In vitro incubation with microsomal preparations from either intestine or liver is one of the most popular approaches to estimate the extent of potential first pass metabolism of the drug candidates.

In summary, the current study is proposed for B7T aiming to understand its extent and rate of oral absorption, intestinal transport mechanisms as well as potential intestinal and hepatic metabolisms. The present study plans to investigate intestinal absorption of B7T using epithelium-mimic artificial membrane, Caco-2 cell monolayer model and single-pass intestinal perfusion model. In addition, in vitro metabolism with organ-derived sub-cellular fractions will be conducted to estimate intestinal and hepatic first-pass effects of B7T.

2. Materials and methods

2.1. Materials

Bis(7)-tacrine dihydrochloride was synthesized as described previously (Pang et al., 1996). Pimozide used as internal standard (IS) for analysis of blood samples was purchased from Sigma Chemical Co. (St. Louis, MO, USA) (Fig. 1). Lornoxicam, as IS for analysis for all the in vitro samples, was purchased from (Iffect Chemphar Co., Hong Kong). Acetonitrile (HPLC grade) were obtained from Labscan (Labscan Asia, Thailand). Phosphate buffered saline tablets were purchased from Sigma Chemical Co. (St. Louis, MO, USA). All of the other reagents were of analytical grade or HPLC grade. Distilled water was used for the preparation of all solutions. For cell culture, Dulbecco's modified Eagle's medium, fetal bovine serum, 0.05% Trypsin–EDTA, Penicillin-Streptomycin, and non-essential amino acids, HBSS buffer were obtained from Gibco BRL (Carlsbad, CA, USA) and Life Technologies (Grand Island, NY, USA).

2.2. Methods

2.2.1. Parallel artificial membrane permeation assay (PAMPA) of B7T at various pHs

The permeabilities of B7T and propranolol (a transcellular marker) were estimated using 96-well MultiScreen^{TM} Permeability Plates (Millipore, USA). Each transwell was coated with 15 μl of a 5% solution of hexadecane in hexane. The artificial membrane was constructed after complete evaporation of hexane. B7T was dissolved in 0.01 M phosphate buffer with 5% DMSO at pH values ranging from 2 to 8. Loading concentra-

tions of B7T were 500 μg/ml at pH from 2.0 to 7.4 and 100 μg/ml at pH 8.0. Propranolol was also prepared in 0.01 M phosphate buffer (pH 6.8 and 7.4) at a concentration of 500 μg/ml. A 150 μl of various drug solutions was added to the donor side of the transwell and 300 μl of 0.01 M phosphate buffer at the corresponding pH was placed in receiver side of the transwell. The permeation assay was conducted at 37 °C for 5 h. At the end of study, 100 and 250 μl of samples were taken from donor and receiver sides of the plate for concentration analysis.

2.2.2. Transport studies in Caco-2 cell model

Caco-2 cells from the American Type Culture Collection were cultured following the condition as described previously (Zhang et al., 2007). The cells harvested were plated onto Transwell® inserts (24 mm ID, 0.4-m pore size, 4.71 cm^2 of growth area, polycarbonate filter, Corning Costar Co., NY) at a density of 3×10^5 cells/well and cultured for 21 days prior to transport experiments. The integrity of the monolayer was monitored by measuring the Transepithelial Electrical Resistance (TEER) at 37 °C with an epithelial voltohmmeter (World Precision instruments, Inc., FL, USA). Only Caco-2 monolayers with TEER above 600 $\Omega \times cm^2$ (after subtracting the background value of the Transwell®) prior to the transport study were employed in the transport study.

The transport study was carried out in HBSS buffer (pH 6.8). Caco-2 cell monolayer grown for 21 days were rinsed twice and equilibrated with HBSS buffer at 37 °C for 15 min before the transport experiment. In the bi-directional transport study, B7T (25 μg/ml) or propranolol (43 μg/ml) in HBSS buffer was loaded onto the apical (AP) (1.5 ml of transport buffer) or basolateral (BL) (2.6 ml of transport buffer) side, the so-called the donor side. Aliquots of 0.5 ml samples were taken from the other side, the so-called receiver side at different time intervals (15, 30, 45, 60, 90, and 120 min) during the experiment. Same volume of blank HBSS buffer was replaced to the receiver chamber after each sampling. Samples taken from the transport study were mixed with 0.1 ml methanol, and then stored at −80 °C until analysis.

To determine the intracellular amount of B7T, the Caco-2 cell monolayers were obtained from the filters of Transwells® after each transport study and rinsed with 50 ml ice-cold saline for three times. Afterward, the collected monolayers spiked with 50 μl of lornoxicam (40 μg/ml, in ACN/acetic acid (9:1 v/v)), the internal standard, were lysed with 3 ml of methanol followed by sonication for 10 min. The lysate was centrifuged at 16,000 × *g* for 10 min. The collected supernatant was then evaporated to dryness in a Centrivap concentrator. The residue was reconstituted with 200 μl of 50% ACN (v/v) in 0.05% formic acid aqueous solution and an aliquot of 100 μl of the mixture was injected into the HPLC for analysis.

2.2.3. Intestinal perfusion of B7T in rat single-pass intestinal perfusion model

The rat single-pass intestinal perfusion model was established as described previously (Zhang et al., 2005). Briefly, male Sprague–Dawley rats (body weight: 280–320 g) were anesthetized by an intramuscular injection of a mixture containing 60 mg/kg ketamine and 6 mg/kg xylazine. During the surgical process, the body temperature was maintained at 37 °C by a heating lamp. Fresh heparinized blood was collected from donor rats by cardiac puncture. Right jugular vein for infusion of donor blood was cannulated with a polyethylene tubing (0.5 mm ID, 1 mm OD, Portex Ltd., Hythe, Kent, England). The infusion rate of donor blood via right jugular vein was set at 0.3 ml/min. The small intestine was then exposed by midline incision, and a 7–11 cm long segment of jejunum cannulated with silicon tubing (2.4 mm ID, 4.0 mm OD) connected to a peristaltic pump. The segment was then flushed with warm saline to remove intestinal contents. The mesenteric vein for collecting blood from the specified segment of intestine was cannulated with a 6 cm long polyethylene tubing (0.86 mm ID, 1.27 mm OD, Portex Ltd., Hythe, Kent, England). The blood was collected into the pre-weighted micro-tubes at every 5 min.

The perfusion buffer (at pH 6.8) was isotonic and composed of 2.7 mM KCl, 1.3 mM KH_2PO_4, 8.1 mM Na_2HPO_4, 0.9 mM $CaCl_2$, 0.4 mM $MgCl_2$, and 0.137 M NaCl at 37 °C. In addition, 50 μg/ml of phenol red was added to the perfusate as a non-absorbable marker. The flow rate of perfusate applied to the lumen was set at 0.3 ml/min.

The perfusate containing 25 μg/ml of B7T was applied to the rat jejunum. Samples obtained from both the outlet of the intestine and the mesenteric vain were collected into the pre-weighted micro-tubes at every 5 min.

2.2.4. Estimation of the binding of B7T towards intestinal tissues and Caco-2 cell lysate

The excised rat intestine and harvested Caco-2 cells were homogenized in 25 mM of Tris (pH 7.4) using Polytron homogenizer (Kinematica, Switzerland), respectively. The protein content of the prepared rat intestine homogenate and Caco-2 lysate were determined by Bio-Rad protein assay kit (Hercules, CA). To evaluate the extent of binding of B7T to intestinal tissue and Caco-2 cell monolayer, 25 μg/ml of B7T was incubated with intestine homogenate (1 mg/ml) or Caco-2 cell lysate (1 mg/ml) for 30 min followed by ultrafiltration with a 30 K MW cutoff filter membrane at 12,000 g (Millipore, USA). The control experiments were carried out for B7T in phosphate buffer saline. The protein binding was calculated using the following equation (Pendyala and Creaven, 1993):

$$\%\ \text{protein binding} = \frac{1 - C_u}{C} \times 100\%$$

where C_u is the concentration from the ultrafiltrate of tissue homogenate or cell lysate and C refers to the concentration obtained from the filtrate of the control.

2.2.5. Investigation of potential intestinal and liver first pass metabolism of B7T

2.2.5.1. In vitro P450 mediated oxidation assay. B7T at a concentration of 50 μg/ml was incubated with rat intestine or liver microsomes, or the 21-day cultured Caco-2 cell lysate (0.5 mg/ml of final protein concentration) at 37 °C in Tris buffer (pH 7.4) containing 8 mM of $MgCl_2$, 25 μg/ml of alamethicin, 1.3 mM $NADP^+$, 3.3 mM glucose-6-phosphate and 0.4 U/ml

glucose-6-phosphate dehydrogenase. The reactions lasted for 30, 60, 90, 120 min or 14 h.

2.2.5.2. In vitro glucuronidation activity assay. B7T at a concentration of 50 μg/ml was pre-incubated with rat liver or intestine microsomes at a final protein concentration of 0.5 mg/ml in 50 mM Tris–HCl buffer (pH 7.4) containing 8 mM of $MgCl_2$ and 25 μg/ml of alamethicin for 10 min at 37 °C. The reaction was initiated by the addition of 2 mM of UDPGA and performed for 30, 60, 90, and 120 min.

All the above metabolic reactions were quenched by adding 40 μl of ice-cold ACN/acetic acid (9:1 v/v) containing 40 μg/ml of lornoxicam (the internal standard). All the experiments were conducted in triplicate.

2.2.6. Sample analysis

2.2.6.1. Determination of the B7T blood concentrations. The blood samples were prepared as described previously (Yu et al., 2007). In brief, a 100 μl of blood sample was spiked with 50 μl of pimozide (60 μg/ml) as the IS and 100 μl of 0.2 M sodium carbonate solution followed by extraction with 1.0 ml of ethyl acetate. Ethyl acetate phase was evaporated to dryness with a Centrivap concentrator. The residue was reconstituted with 100 μl mobile phase and centrifuged at 16,000 × *g* for 10 min. An aliquot of 10 μl of the supernatant was applied to LC-MS/MS for analysis.

The HPLC system is composed of PerkinElmer PE-200 series micro-pumps and auto-sampler (PerkinElmer, Norwalk, CT, USA). The chromatographic separation was achieved by C-18 revered phase HPLC column (150 mm × 2.1 mm ID, 5 μm particle size, Agilent), protected by a guard column (12.5 mm × 2.1 mm ID, 5 μm particle size, Agilent). The HPLC column was eluted by a mixture of 0.05% formic acid in water and acetonitrile (1:1, v/v) at a flow rate of 0.35 ml/min. B7T and IS were analyzed with a PerkinElmer Sciex API Q-Trap (Applied Biosystems, Toronto, Canada) as described previously (Zhang et al., 2008). The mass spectrometer was operated using electrospray ionization in positive mode with the following parameters (ionspray voltage: 5500 V, declustering potential: 39 V, entrance potential: 9 V, collision cell exit potential: 4 V, collision energy: 39 V, curtain gas: 40 psi, nebulizer gas: 50 psi, auxiliary gas: 80 psi, and source temperature: 400 °C). Quantitative determination of B7T was performed by using the instrument in the multiple reaction monitoring (MRM) mode to measure the following ion transitions: *m/z* 247 $[M+2H]^{2+}$ to *m/z* 197 (product ion) for B7T and *m/z* 462 $[M+H]^{+}$ to *m/z* 328 (product ion) for IS.

2.2.6.2. Determination of B7T from in vitro samples. All the collected in vitro samples were injected into HPLC for analysis without any further treatment. Due to relative high concentrations of B7T in the in vitro samples, HPLC coupled with UV detector was used for its determination. The HPLC system is composed of Waters 600 controller (pump), Waters 717 auto sampler and Waters 2487 dual wavelength detector. An aliquot of 100 μl of in vitro sample was separated with C-18 revered phase HPLC column (250 mm × 4.6 mm ID, 5 μm particle size, Agilent) eluted by a mobile phase gradient at a flow rate of 1 ml/min. The gradient began with 75% of eluent A (0.5% TEA in water adjusted to pH 3.0 with concentrated phosphoric acid) and 25% of eluent B, ACN and changed linearly to 40% A, 60% B in 0–5 min; then 40% A, 60% B in 5–8 min; and then back to the initial composition in 1 min followed by 6 min equilibrium. B7T was detected at the wavelength of 336 nm.

2.2.7. Data analysis

2.2.7.1. Calculation of the B7T permeabilities in PAMPA. The permeabilities of B7T and propranolol across artificial membrane were calculated as Eq. (1) (Wohnsland and Faller, 2001):

$$P_e = \frac{V_D \times V_R}{(V_D + V_R) \times A \times T} \times \left[-\ln\left(1 - \frac{C_R}{C_{eq}}\right)\right] \quad (1)$$

where V_R is the volume of the receiver compartment (0.3 cm^3), V_D is the donor volume (0.15 cm^3), A is the area of artificial membrane and T is the incubation time (5 h). C_R is the drug concentration in the receiver compartment after 5 h-transport study. C_{eq} is the theoretical drug concentration in the receiver compartment after full equilibrium of the drug between donor and receiver compartment.

2.2.7.2. Calculation of the B7T permeabilities in Caco-2 cell model. The permeability coefficient (P_{app}) of B7T in Caco-2 cell model was calculated as described previously (Artursson and Karlsson, 1991).

$$P_{app} = \frac{dC/dt \times V}{A \times C} \quad (2)$$

where "dC/dt" is the change of the drug concentration in the receiver chambers over time, "V" is the volume of the solution in the receiver chambers (cm^3); "A" represents the membrane surface area (cm^2); "C" is the initial concentration in the donor chambers.

In addition, the recoveries of studied compounds were calculated using Eq. (3):

$$\text{Recovery}\,(\%) = \frac{\text{Sum of the compound in both donor and receiver chamber after transport study}}{\text{The initial amount of the compound loaded in the donor chamber}} \times 100\% \quad (3)$$

2.2.7.3. Calculation of the B7T permeabilities in rat single-pass intestinal perfusion model. The concentration of the analytes in the perfusate was corrected for the water flux as Eq. (4) before other calculations were performed (Cummins et al., 2003):

$$\text{Conc}_{\text{corrected}} = \text{Conc}_{\text{measured}} \times \frac{(\text{Phenol red})_{\text{in}}}{(\text{Phenol red})_{\text{out}}} \quad (4)$$

The permeability coefficients of compounds based on the appearance of the compounds in the mesenteric blood (P_{Blood}) and the disappearance of the compounds in the perfusate (P_{Lumen}) were calculated according to Eq. (5) (Amidon et al.,

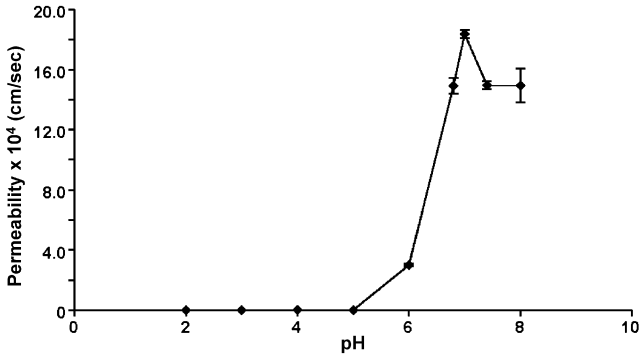

Fig. 2. Permeability of B7T across artificial membrane at various pH.

1980; Johnson et al., 2003) and Eq. (6) (Cummins et al., 2003), respectively.

$$P_{\text{Blood}} = \frac{dX/dt}{AC_0} \quad (5)$$

where dX/dt is the rate of drug appearing in mesenteric blood, A is the area of the intestine segment. C_0 is the initial drug concentration in the perfusate.

$$P_{\text{Lumen}} = -\frac{Q}{2\pi rl}\ln\frac{C_{\text{out}}}{C_{\text{in}}} \quad (6)$$

where r is the radius of the perfused intestinal segment and l is the length of the perfused intestinal segment. Q is the perfusate flow rate. C_{in} is the drug concentration in the inlet of the perfusate entering the intestinal segment. C_{out} is the drug concentration in the exiting perfusate at the steady state.

Intestinal extraction ratio (ER) was estimated following Eq. (7) (Cummins et al., 2003):

$$\text{ER} = 1 - \frac{P_{\text{Blood}}}{P_{\text{Lumen}}} \quad (7)$$

2.2.8. Statistical analysis

Statistically significant differences between two groups or more than two groups were evaluated by Student's t-test and one-way ANOVA, respectively. A $P < 0.05$ was considered significant for all tests.

3. Results

3.1. Permeation of B7T in PAMPA

As an organic base, the permeability of B7T varied substantially from pH 2 to 8 (Fig. 2). Under acidic conditions (pH 2–5), there were no B7T detected at the receiver side in the period of 5-h permeation study. Based on the detection limit of B7T (50 ng/ml), its permeability was estimated to be lower than 6.3×10^{-9} cm/s. Along with the increase of pH, the permeabilities of B7T were elevated rapidly from pH 5.0 and reached the plateaus at pH 7–8. In summary, the pH-permeability profile of B7T seemed to follow pH-partition hypothesis. The permeability at physiological pH of bio-fluid (pH 7.4) and pH of intestinal fluid (pH 6.8) were $1.50 \pm 0.03 \times 10^{-5}$, and $1.49 \pm 0.05 \times 10^{-5}$ cm/s, respectively. It is expected that amount of the unionized form of B7T, which are more rapidly diffused across biological membranes, will be increased with the pH. Comparison of permeability of B7T with propranolol, the well-known transcellular marker, at pH 7.4 and 6.8 ($2.58 \pm 0.07 \times 10^{-5}$, $2.76 \pm 0.08 \times 10^{-5}$ cm/s, respectively for propranolol) demonstrated that the permeabilities of both compounds were higher than 1.0×10^{-5} cm/s indicating their readiness of crossing artificial membrane.

3.2. Transport of B7T in Caco-2 cell model

Although the permeability of B7T was comparable to propranolol in PAMPA, permeabilities of B7T in both AP to BL and BL to AP directions were only 14% and 21% of that of propranolol, respectively (Fig. 3). In addition, the bi-directional transport of B7T resulted in similar P_{app} values, indicating the lack of involvement of active transporters in the absorption or disposition during its absorption process (Fig. 3). Surprisingly, the recoveries in bi-directional transport of B7T were much lower (AP to BL: $36.0 \pm 3.8\%$; BL to AP: $66.4 \pm 10.9\%$) than that of propranolol ($91.9 \pm 3.4\%$). After the further analyses of the intracellular amount of B7T, it was found that there were 21.1 ± 1.0 and 18.8 ± 1.8 μg of B7T accounting for over 56% and 29% of the related loading dose being trapped in the Caco-2 cell monolayer during its AP to BL and BL to AP transport, respectively. The high affinity of B7T to the intracellular content was further confirmed in binding study for B7T. It was shown that $98.7 \pm 0.3\%$ of B7T was bound to the Caco-2 cell lysate, which may result in its significant cellular uptake. Further analyses also revealed that there is no metabolite for B7T found during its 2-h transport study and most of B7T ($97.8 \pm 1.8\%$) still remained in the metabolic reaction system after 14-h incubation with Caco-2 cell lysate.

3.3. Rat in situ intestinal perfusion study of B7T

The cumulative amount of B7T in the mesenteric blood increased linearly with the time of perfusion (Fig. 4). Permeability coefficient (P_{Lumen}) based on the disappearance of B7T in the intestine lumen was calculated to

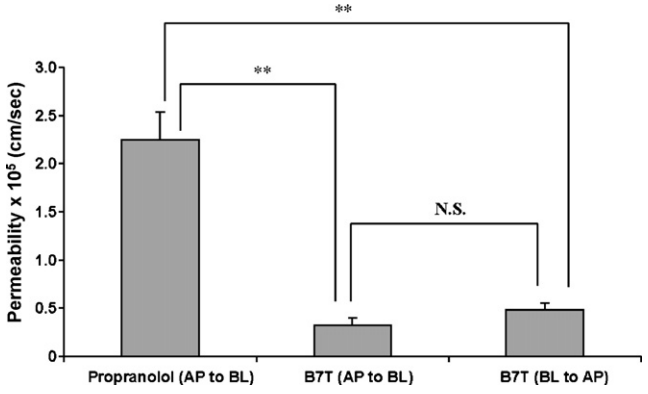

Fig. 3. Permeabilities of B7T and propranolol across Caco-2 cell monolayer ($N = 3$). Data express as mean ± S.D. $^{**}P < 0.01$. N.S.: no significance.

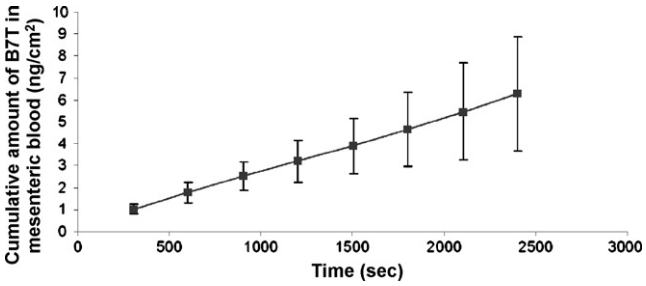

Fig. 4. Cumulative amount of B7T appearing in the mesenteric blood over time in the rat jejunum single-pass perfusion study. Data express as mean ± S.D. ($N = 5$).

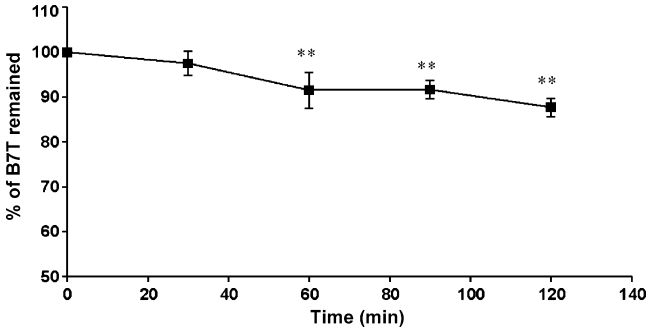

Fig. 5. Percentage of B7T remained during 2-h in vitro incubation with rat liver microsome. Data express as mean ± S.D. $N = 3$. $^{**}P < 0.01$.

be $3.79 \pm 1.89 \times 10^{-5}$ cm/s, which was significantly lower than the reported values for those of well-absorbed markers such as, antipyrine ($P_{Lumen} = 1.867 \times 10^{-4}$ cm/s) and glucose ($P_{Lumen} = 2.817 \times 10^{-4}$ cm/s), implying a much less efficient intestine absorption of B7T (Wang et al., 1997). In addition, the calculated P_{Blood} ($1.02 \pm 0.43 \times 10^{-7}$ cm/s) was also poor, which further confirms the difficulty of B7T crossing intestinal epithelium. Based on the P_{Blood} and P_{Lumen} of B7T, the ER of B7T was estimated to be 99.7%, which suggested that most of B7T was extracted by intestine during its absorption process. Such high ER could be explained by the high affinity of B7T towards the intestine, which was further supported by its extremely high intestinal tissue-binding ratio ($99.9 \pm 0.03\%$). Consistent with the findings from Caco-2 model, there is no metabolite of B7T found in both mesenteric blood and perfusate.

3.4. Liver and intestinal metabolism of B7T

3.4.1. In vitro P450 mediated oxidation assay

B7T was stable in the presence of the NADPH during 2-h incubation with rat intestinal microsome and there were $96.6 \pm 3.5\%$ of B7T remained even after 14-h incubation. However, the amount of B7T was gradually reduced when it is incubated with rat liver microsome in the presence of NADPH (Fig. 5). It was found that there was $24.2 \pm 2.1\%$ of B7T metabolized in 14 h. Three metabolites, namely M1, M2 and M3, with the similar UV spectra of B7T, were found (Fig. 6). These metabolites of B7T were further identified with LC/MS/MS. B7T, as a dimeric tacrine analog, was preferentially double-charged. Besides the protonated molecular ion of $[M+H]^+$ at m/z 493, base peak $[M+2H]^{2+}$ appeared at m/z 247 (Fig. 7).

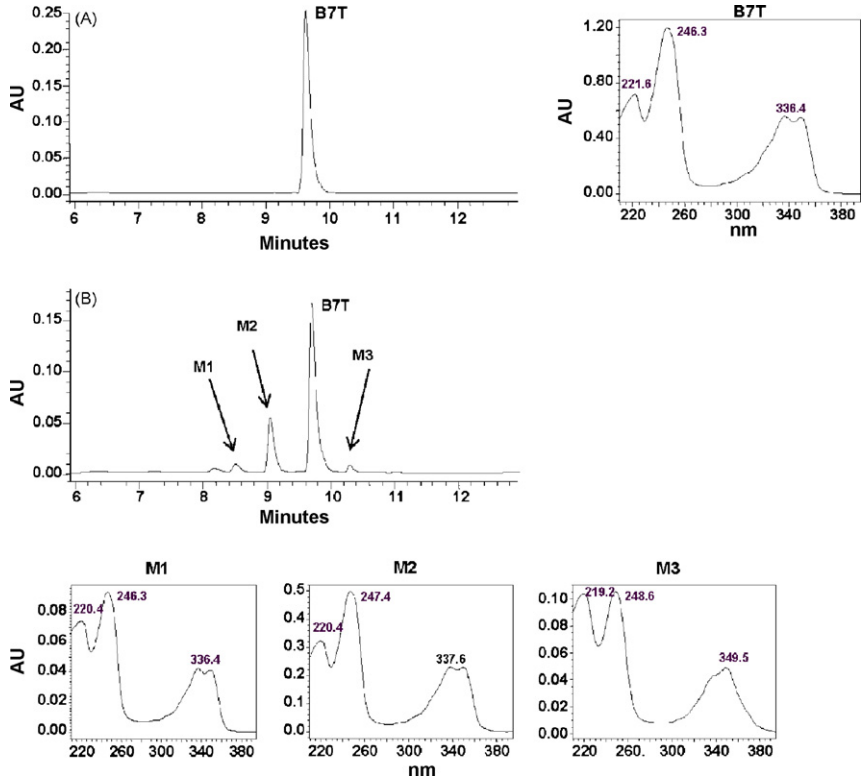

Fig. 6. HPLC/UV chromatogram of the samples obtained after 14-h incubation with rat liver microsome in absence (A) and presence (B) of NADPH.

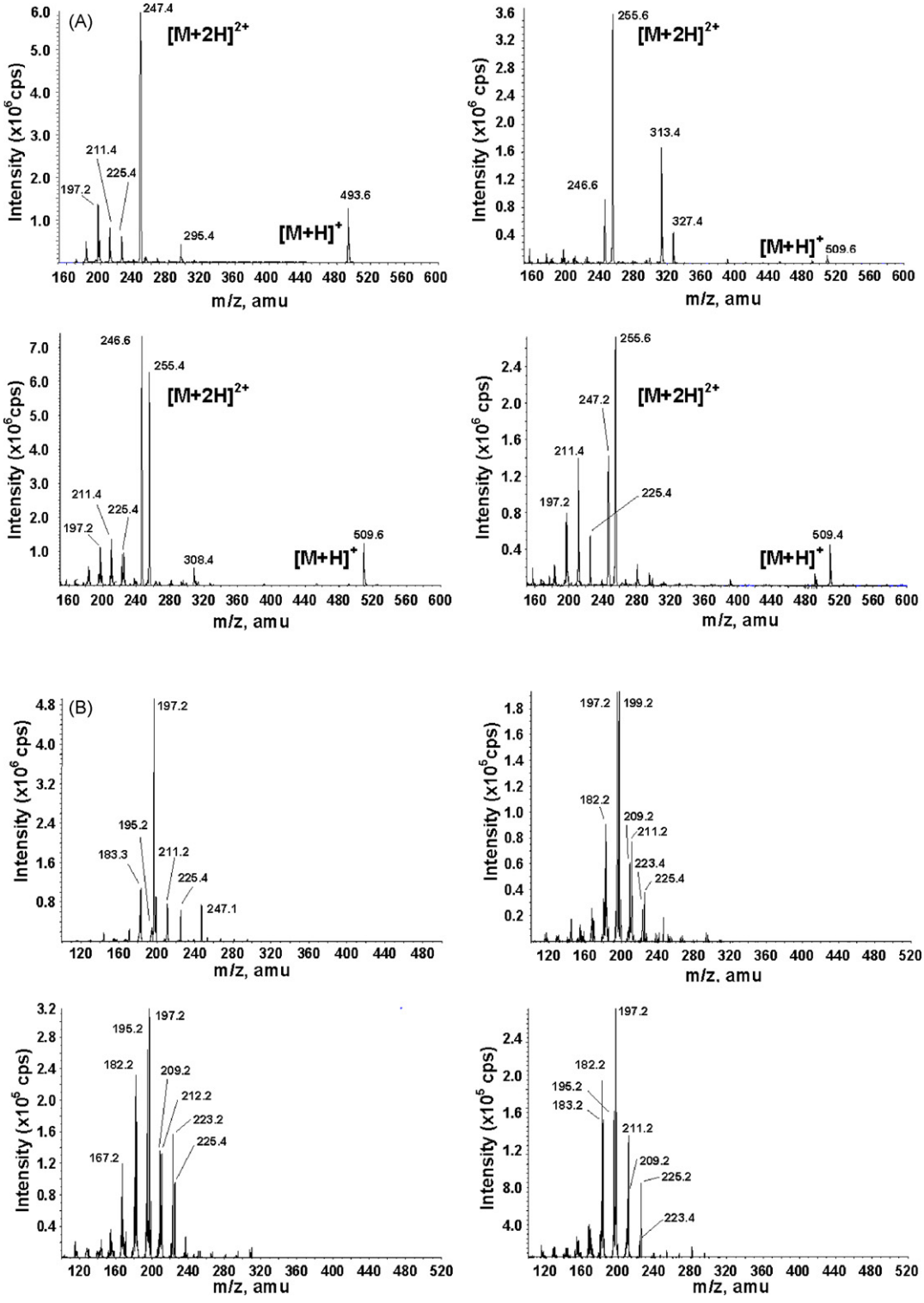

Fig. 7. The mass spectra (A) and product ion spectra (B) of B7T and its metabolites.

The base peak $[M+2H]^{2+}$ was further bombarded by collision energy to provide the product ion spectrum of B7T. The protonated molecule preferentially generated fragment ion of *m/z* 197, corresponding to the moiety of tacrine. Fragmentation also occurred at the α-C or β-C of heptylene chain of B7T resulting in fragment ions at *m/z* 211 and *m/z* 225, respectively (Fig. 8). The lower ion intensity of the two fragment ions at *m/z* 211 and *m/z* 225 relative to that at *m/z* 197 may probably result from the preferential dissociation taking place at the more polarized N–C bond rather than C–C bond. The molecular ions of the three metabolites $[M+H]^+$ was at *m/z* 509 indicating their possible identities as hydroxylation products of B7T. Like their

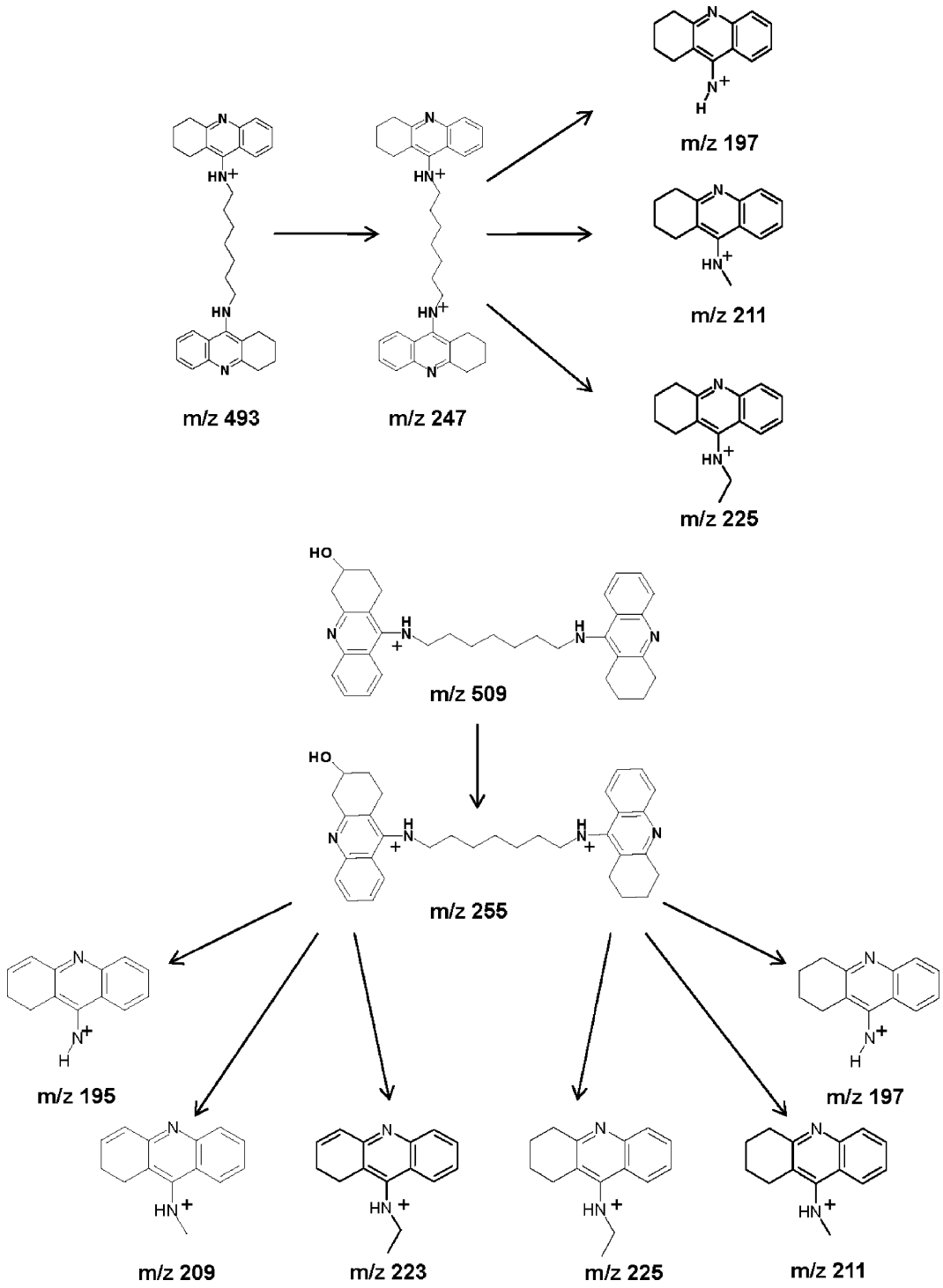

Fig. 8. Postulated fragmentation pathway of B7T (above) and its hydroxylated metabolite (bottom) in positive ion mode.

parent, the metabolites were readily double-charged resulting in base peak $[M+2H]^{2+}$ at *m/z* 255. $[M+2H]^{2+}$ was prone to lose –OH to produce $[M+2H-OH]^{2+}$ at *m/z* 246 even under no collision energy (Fig. 7). M1 seemed to be labile during Q1 scan and lost tacrine and methylene tacrine moiety generating ions at *m/z* 327and *m/z* 313, which were not found in the mass spectra of M2 and M3. The fragmentation spectra of $[M+2H]^{2+}$ of metabolites at *m/z* 255 provide more information on their chemical structures. As shown in the spectra, the product ions of the metabolites were the sum of the fragments from two parts of tacrine in B7T with and without hydroxylation. The part of the molecules without hydroxylation generated the fragments identical to product ions of B7T, i.e. the ions at *m/z* 197, *m/z* 211, *m/z* 225, etc. On the other hand, the part of hydroxylated tacrine of the metabolites produced its fragments with their *m/z* at 2 mass units less than their counterparts of tacrine moiety without hydroxylation at the other end of the molecule, i.e. *m/z* 195, *m/z* 209, *m/z* 223 as deduced in Fig. 8.

In the first step, dehydration took place at the cyclohexane of hydroxylated metabolites in the period of Q3 scanning by forming cyclohexene ring with 2 mass units less than B7T. Then, the dehydrated metabolites followed the exact fragmentation pattern as B7T resulting in ions at *m/z* 195, *m/z* 209, and *m/z* 223, respectively.

3.4.2. In vitro glucuronidation assay

Since glucuronidation may take place at amine group (Woolf, 1999), we also investigated the potential glucuronidation of B7T by liver and intestine microsome. The result showed that there is no significant glucuronidation occurred when B7T was incubated with either liver or intestine microsome.

4. Discussions

B7T, the novel synthetic tacrine analog, is our recently developed acetylcholinesterase inhibitor for the treatment of Alzheimer's disease. Quite a number of studies from us have demonstrated its potent biological activities (Wu et al., 2000; Li et al., 2005, 2006). However, there is a lack of information on its pharmacokinetic properties. Our pilot study indicated that less than 5% of B7T appeared in blood circulation after its oral administration to rats. With a very high lipophilicity (Log *P* of 8.2) (Yu et al., 2008), B7T is expected to easily traverse intestinal epithelium. The potential low oral bioavailability for such a highly lipophilic drug inspired our curiosity on the further investigation of its biopharmaceutics and pharmacokinetics characteristics. Therefore, we employed various intestinal absorption models and in vitro metabolism approaches to estimate the extent of intestinal absorption of B7T and first-pass effects rendered by liver and intestine. The current study is our first preclinical investigation on the intestinal absorption and metabolism of B7T. Since we have a series of novel AChEIs which are synthesized as homo- or hetero-dimeric AChEIs that contain tacrine according to the computer docking-studies, we do hope the current study would also serve as a systematic screening approach to find the potential good candidates that own better biopharmaceutics and pharmacokinetics properties for further in vivo clinical study.

In PAMPA model, the rapid permeability coefficients ($>10^{-5}$ cm/s) of B7T at both pH 7.4 and 6.8 suggested that it might own promising permeability across the intestinal epithelium in vivo. As PAMPA is only non-cell based assay, further assay using Caco-2 cell model was subsequently carried out. However, the absorptive permeability of B7T across Caco-2 cell monolayer was substantially reduced comparing with that found in PAMPA. Several reasons were suspected, including high cell uptake, extensive intestinal first-pass metabolism and involvement of efflux transport. Unlike the high recovery found in PAMPA (>90%), a much lower recovery of B7T ($36.0 \pm 3.8\%$) after transport study in Caco-2 cell model was observed. By determining the amount of cellular uptake of B7T, it was found that about 57% of it was trapped inside the Caco-2 cells during its transport process in the Caco-2 monolayer model. Consistently, the extensive binding (over 98%) was found when B7T was incubated with Caco-2 lysate. On the other hand, metabolism in Caco-2 cells should not play a role in the low permeability of B7T since no appreciable metabolism was observed in both 2-h Caco-2 transport study and 14-h in vitro incubation with Caco-2 cell lysate. Although Caco-2 cell monolayer cultured for 21 days was reported to express various efflux transporters such as P-gp, MRPs, MXT (Saitoh and Aungst, 1995; Hirohashi et al., 2000; Gutmann et al., 2005), P_{app} of B7T from AP to BL and from BL to AP was similar, implying that B7T was mainly transported through the passive diffusion pathway. Thus, efflux transport may not contribute to the low absorptive P_{app} of B7T. Since first pass metabolism and efflux transport had little impact on absorption of B7T, extensive cellular uptake seemed to be the major cause responsible for the significantly lower P_{app} of B7T in Caco-2 cell model than that in PAMPA.

In order to mimic the in vivo situation, rat single-pass intestinal perfusion model was used with simultaneous monitoring of B7T in both perfusate and mesenteric blood. In spite of less efficient absorption of B7T than that of high oral bioavailability marker (such as antipyrine and glucose), B7T should have a moderate extent of absorption estimated from its P_{Lumen} value. However, extremely low P_{Blood} was detected. For comparison purpose, the current single-pass intestinal perfusion studies were carried out by measuring both the disappearance of the B7T from the perfusate and appearance of B7T in the mesenteric blood analysis. Based on the data obtained, if permeability of B7T was only estimated with perfusate measurement and neglected the amount of B7T present in the mesenteric blood, the calculated P_{Lumen} ($3.79 \pm 1.89 \times 10^{-5}$ cm/s) would overestimate the extent of B7T intestinal absorption. In the mean time, the great difference between P_{Lumen} and P_{Blood} of B7T actually indicates the potential extensive intestinal extraction of B7T. However, such high intestinal extraction may not be due to the extensive intestinal metabolism of B7T, since there is no metabolite found in both perfusate and mesenteric blood. Moreover, the in vitro incubation of B7T with intestinal microsome did not indicate its extensive intestinal metabolism either. Therefore, the high intestinal extraction of B7T may be mainly due to its significant intestinal tissue binding ($99.9 \pm 0.03\%$ of B7T binding with intestinal tissue).

The current study for the first time reveal the formation of metabolites of B7T, though the positions of hydroxylation have not been confirmed. Previously, the hydroxylation of tacrine was reported to preferentially take place at its 1, 2, 4 position (Hsu et al., 1990). Further study should be performed to clarify whether the hydroxylation of B7T has the similar position preference as tacrine.

5. Conclusion

The intestinal absorption of B7T, a novel acetylcholinesterase inhibitor, is not remarkable. Passive diffusion seems to be the main transport pathway for B7T across intestinal epithelium. Extensive intestinal extraction in vivo due to significant tissue binding gives rise to the poor intestinal permeability of B7T, which may further contributes to its low oral bioavailability. Although metabolism in intestine was not significant, hepatic

metabolism of B7T may also play a role in its low oral bioavailability in vivo.

Acknowledgements

This work was kindly supported by the Research Grants Council of Hong Kong (HKUST 6133/03M, 6441/06M, 6608/07M and N_PolyU 618/07) and Macao Science & Technology Development Fund (Ref. No. 049/2005/A-R10). We would also like to thank our benefactors for the generous financial and material supports.

References

Amidon, G.L., Leesman, G.D., Elliott, R.L., 1980. Improving intestinal absorption of water-insoluble compounds: a membrane metabolism strategy. J. Pharm. Sci. 69, 1363–1368.

Artursson, P., Karlsson, J., 1991. Correlation between oral drug absorption in humans and apparent drug permeability coefficients in human intestinal epithelial (Caco-2) cells. Biochem. Biophys. Res. Commun. 175, 880–885.

Bird, T.D., 1998. Alzheimer's disease and other primary dementias. In: Harrison's Principles of Internal Medicine, 14th ed. McGraw-Hill, New York, p. 2348.

Cummins, C.L., Salphati, L., Reid, M.J., Benet, L.Z., 2003. In vivo modulation of intestinal CYP3A metabolism by P-glycoprotein: studies using the rat single-pass intestinal perfusion model. J. Pharmacol. Exp. Ther. 305, 306–314.

Gutmann, H., Hruz, P., Zimmermann, C., Beglinger, C., Drewe, J., 2005. Distribution of breast cancer resistance protein (BCRP/ABCG2) mRNA expression along the human GI tract. Biochem. Pharmacol. 70, 695–699.

Hirohashi, T., Suzuki, H., Chu, X.Y., Tamai, I., Tsuji, A., Sugiyama, Y., 2000. Function and expression of multidrug resistance-associated protein family in human colon adenocarcinoma cells (Caco-2). J. Pharmacol. Exp. Ther. 292, 265–270.

Hsu, R.S., Shutske, G.M., Dileo, E.M., Chesson, S.M., Linville, A.R., Allen, R.C., 1990. Identification of the urinary metabolites of tacrine in the rat. Drug Metab. Dispos. 18, 779–783.

Johnson, B.M., Chen, W.Q., Borchardt, R.T., Charman, W.N., Porter, C.H., 2003. A kinetic evaluation of the absorption, efflux, and metabolism of verapamil in the autoperfused Rat Jejunum. J. Pharmacol. Exp. Ther. 305, 151–158.

Li, W., Lee, N.T., Fu, H., Kan, K.K., Pang, Y., Li, M., Tsim, K.W., Li, X., Han, Y., 2006. Neuroprotection via inhibition of nitric oxide synthase by bis(7)-tacrine. Neuroreport 17, 471–474.

Li, W., Pi, R., Chan, H.H., Fu, H., Lee, N.T., Tsang, H.W., Pu, Y., Chang, D.C., Li, C., Luo, J., Xiong, K., Li, Z., Xue, H., Carlier, P.R., Pang, Y., Tsim, K.W., Li, M., Han, Y., 2005. Novel dimeric acetylcholinesterase inhibitor bis(7)-tacrine, but not donepezil, prevents glutamate-induced neuronal apoptosis by blocking *N*-methyl-D-aspartate receptors. J. Biol. Chem. 280, 18179–18188.

Nordberg, A., Svensson, A.L., 1998. Cholinesterase inhibitors in the treatment of Alzheimer's disease: a comparison of tolerability and pharmacology. Drug Safety 19, 465–480.

Paine, M.F., Fisher, M.B., 2000. Immunochemical identification of UGT isoforms in human small bowel and in Caco-2 cell monolayers. Biochem. Biophys. Res. Commun. 273, 1053–1057.

Pang, Y.P., Quiram, P., Jelacic, T., Hong, F., Brimijoin, S., 1996. Highly potent, selective, and low cost bis-tetrahydroaminacrine inhibitors of acetylcholinesterase. Steps toward novel drugs for treating Alzheimer's disease. J. Biol. Chem. 271, 23646–23649.

Pendyala, L., Creaven, P.J., 1993. In vitro cytotoxicity, protein binding, red blood cell partitioning, and biotransformation of oxaliplatin. Cancer Res. 53, 5970–5976.

Saitoh, H., Aungst, B.J., 1995. Possible involvement of multiple Pgp-mediated efflux systems in the transport of verapamil and other organic cations across rat intestine. Pharm. Res. 12, 1304–1310.

Standridge, J.B., 2004. Pharmacotherapeutic approaches to the treatment of Alzheimer's disease. Clin. Ther. 26, 615–630.

Sun, D., Lennernas, H., Welage, S.L., Barnett, J.L., Landowski, C.P., Foster, D., Fleisher, D., Lee, K.D., Amidon, G.L., 2002. Comparison of human duodenum and Caco-2 gene expression profiles for 12,000 gene sequences tags and correlation with permeability of 26 drugs. Pharm. Res. 19, 1400–1416.

Tariot, P., 2001. Current status and new developments with galantamine in the treatment of Alzheimer's disease. Expert Opin. Pharmacother. 2, 2027–2049.

Wang, H., Carlier, P.R., Ho, W.L., Wu, D.C., Lee, N.T., Li, C.P., Pang, Y.P., Han, Y.F., 1999. Effects of bis(7)-tacrine, a novel anti-Alzheimer's agent, on rat brain. AChE Neuroreport 10, 789–793.

Wang, Y., Aun, R., Tse, F.L., 1997. Absorption of D-glucose in the rat studied using in situ intestinal perfusion: a permeability-index approach. Pharm. Res. 14, 1563–1567.

Watkins, P.B., Zimmerman, H.J., Knapp, M.J., Gracon, S.I., Lewis, K.W., 1994. Hepatotoxic effects of tacrine administration in patients with Alzheimer's disease. JAMA 271, 992–998.

Wilkinson, D.G., Francis, P.T., Schwam, E., Payne-Parrish, J., 2004. Cholinesterase inhibitors used in the treatment of Alzheimer's disease: the relationship between pharmacological effects and clinical efficacy. Drugs Aging 21, 453–478.

Wohnsland, F., Faller, B., 2001. High-throughput permeability pH profile and high-throughput alkane/water log *P* with artificial membranes. J. Med. Chem. 44, 923–930.

Woolf, T.F., 1999. Handbook of Drug Metabolism. Dekker, New York, p. 157.

Wu, D.C., Xiao, X.Q., Ng, A.K., Chen, P.M., Chung, W., Lee, N.T., Carlier, P.R., Pang, Y.P., Yu, A.C., Han, Y.F., 2000. Protection against ischemic injury in primary cultured astrocytes of mouse cerebral cortex by bis(7)-tacrine, a novel anti-Alzheimer's agent. Neurosci. Lett. 288, 95–98.

Xiao, X.Q., Lee, N.T., Carlier, P.R., Pang, Y.P., Han, Y.F., 2000. Bis(7)-tacrine, a promising anti-Alzheimer's agent, reduces hydrogen peroxide-induced injury in rat pheochromocytoma cells: comparison with tacrine. Neurosci. Lett. 290, 197–200.

Yu, H., Ho, J.M.K., Kan, K.K.W., Cheng, B.W.H., Li, W.M., Zhang, L., Lin, G., Pang, Y.P., Gu, Z.M., Chan, K., Wang, Y.T., Han, Y.F., 2007. Development of a high performance liquid chromatography-tandem mass method for determination of bis(7)-tacrine, a promising anti-Alzheimer's dimer, in rat blood. J. Pharm. Biomed. Anal. 44, 1133–1138.

Yu, H., Li, W.M., Kan, K.K.W., Ho, J.M.K., Carlier, P.R., Pang, Y.P., Gu, Z.M., Chan, K., Zuo, Z., Wang, Y.T., Han, Y.F., 2008. The physicochemical properties and the in vivo AChE inhibition of two potential anti-Alzheimer agents, bis(12)-hupyridone and bis(7)-tacrine. J. Pharm. Biomed. Anal. 46, 75–81.

Zhang, L., Lin, G., Chang, Q., Zuo, Z., 2005. Role of intestinal first-pass metabolism during the absorption process of baicalein. Pharm. Res. 22, 1050–1058.

Zhang, L., Lin, G., Kovács, B., Jani, M., Krajcsi, P., Zuo, Z., 2007. Mechanistic study on the intestinal absorption and disposition of baicalein. Eur. J. Pharm. Sci. 31, 221–231.

Zhang, L., Yu, H., Li, W.M., Cheung, M.C., Pang, Y.P., Lin, G., Wang, Y.T., Zuo, Z., Han, Y.F., 2008. Selective and sensitive determination of Bis(7)-tacrine, a high erythrocyte binding acetylcholinesterase inhibitor, in rat plasma by high performance liquid chromatography–tandem mass spectrometry. Biomed. Chromatogr. 22, 414–420.